Calcium-dependent conformational stability of modules 1 and 2 of human gelsolin

André ZAPUN[1], Stéphane GRAMMATYKA, Gaël DÉRAL and Thierry VERNET

Institut de Biologie Structurale J.-P. Ebel (CEA, CNRS, UJF), Laboratoire d'Ingénierie des Macromolécules, 41 rue Jules Horowitz, 38027 Grenoble, France

Gelsolin modulates the actin cytoskeleton in the cytoplasm and clears the circulation of stray filaments. *In vitro*, gelsolin cleaves, nucleates and caps actin filaments, activities that are calcium-dependent. Both cellular and secreted forms share a sequence of 730 residues comprising six homologous modules termed G1–G6. A disulphide bond is formed in secreted G2, whereas in the cytoplasm it remains reduced. A point mutation in G2 causes an amyloidosis with neurological, ophthalmological and dermatological symptoms. This mutation does not affect the cytoplasmic form, while the secreted form is proteolysed. As a first step towards understanding how gelsolin folds and functions in different cellular compartments, we have characterized at equilibrium the urea-induced unfolding of G1 and G2, with or without calcium and/or disulphide bond. G1 and G2 both exhibit two-state unfolding behaviour and are stabilized by calcium. The disulphide bond also contributes to the stability of G2. In the absence of Ca^{2+} and disulphide bond, G2 adopts a non-native conformation, suggesting that folding of G2 in the cytoplasm relies on the presence of surrounding modules or other molecular partners.

Key words: amyloidosis, disulphide bond, protein folding.

INTRODUCTION

Gelsolin exists in a cytoplasmic form, which modulates the actin cytoskeleton and plays a role in cell motility and apoptosis [1–3], and a circulating form, which clears the circulation of potentially dangerous actin filaments [4]. *In vitro*, gelsolin cleaves, nucleates and caps the barbed ends of actin filaments, activities that are calcium-dependent [5]. Both cellular and secreted forms are the product of the same gene and result from alternative splicing; they share a common sequence of 730 residues comprising six homologous modules of about 120 residues, termed G1–G6 [6]. Interestingly, a disulphide bond is formed between Cys-188 and Cys-201 of G2 in the secreted form, whereas the cytoplasmic form remains reduced [7].

The crystallographic structure of equine plasma gelsolin in the absence of calcium is compact and shows intimate interactions between the modules [8]. G1 is sandwiched between G2 and G3, which are connected over G1 by an extended stretch of 30 residues. G1 has extensive contact surfaces with its two surrounding modules. The same organization is repeated with the triplet G4–G6. In the presence of Ca^{2+}, this compact arrangement is thought to relax, thus unmasking actin-binding surfaces [8]. The structure of G4–G6 of human gelsolin bound to G-actin and calcium has recently confirmed that large rearrangements do occur, as G6 does not interact with G4 in this complex [9]. Folding of gelsolin is of particular interest as it occurs in two different cellular compartments. In the cytoplasm, where free Ca^{2+} concentration is normally low, folding produces a presumably inactive native protein, which can then be activated by an increase in calcium concentration. Folding of the secreted form must take place in the endoplasmic reticulum, where the free Ca^{2+} concentration (100–700 μM) [10] should be sufficient to generate directly the active, relaxed form. Does folding occur in the same way in these various environments, with and without calcium, with and without disulphide bond? Do the different modules fold autonomously and then assemble to form the compact structure observed in the absence of calcium, or have they evolved a degree of folding cooperativity as observed with other modular proteins [11]?

Studying the folding of gelsolin will also help understand the molecular mechanisms underlying amyloid diseases. A point mutation in gelsolin was found to be the cause of the familial amyloidosis Finnish type [12]. This autosomal dominant genetic disease manifests itself by neurological, ophthalmological and dermatological symptoms [13]. The Asp-187 of G2 is replaced by either an Asn or a Tyr. The Asp → Asn mutation is the most common and affects about 1000 people in Finland. This mutation does not seem to affect the activity of the cytoplasmic form [14], while the secreted form is proteolysed, possibly both in the secretory pathway and the extracellular medium [15]. The resulting fragment, corresponding to residues 174–247, forms amyloid plaques in patient tissues [16]. The different concentrations of calcium and the formation or absence of the disulphide bond may contribute to the very different fates of the secreted and cytoplasmic forms of the mutated gelsolin.

As a first step towards addressing these questions, we have characterized at equilibrium the urea-induced unfolding of G1 and G2, in the absence and presence of Ca^{2+}. The effect of the disulphide bond on the stability of G2 has also been investigated. G1 and G2 were both found to exhibit a two-state unfolding behaviour and to be stabilized by calcium. The disulphide bond also contributes to the conformational stability of G2. In the absence of both Ca^{2+} and the disulphide bond, G2 adopts a non-native conformation characteristic of a molten globule, suggesting that folding of this module in the cytoplasm relies on the presence of the surrounding modules or other molecular partners. Indeed, within the bimodule G1–G2, the conformation of reduced G2 in the absence of calcium appears to be more native-like, although the stabilization is only marginal.

Abbreviations used: DTT, dithiothreitol; SP-Sepharose, sulphopropyl-Sepharose.

[1] To whom correspondence should be addressed (e-mail andre.zapun@ibs.fr).

EXPERIMENTAL

Chemicals

Ultrapure urea was obtained from ICN Biomedicals; all other chemicals were of analytical grade. Restriction enzymes and their appropriate buffers were from Promega. Oligonucleotides were supplied by Eurogentec.

Cloning and mutagenesis

Plasmids were derived from the expression plasmid pET-3a containing a cDNA encoding human plasma gelsolin (generously provided by H. L. Yin; [17]). The *Eco*RI–*Hin*dIII fragment from the pUC-f1 plasmid (Pharmacia) containing the phage f1 origin of replication was introduced between the corresponding restriction sites of the expression plasmid to allow production of single-stranded DNA for mutagenesis. Site-directed mutagenesis was performed according to [18]. N-terminal deletions were obtained with oligonucleotides corresponding to the desired N-terminal sequence and to the pET-3a sequence upstream of the initial ATG. Stop codons were introduced by point mutations.

Expression and purification

For bacterial expression, plasmids encoding both variants of G1 were transformed into *Escherichia coli* BL21(DE3). Plasmids encoding the variants of G2 and the bimodule G1–G2 were transformed in the same strain containing the plasmid pLysS. Expression was induced at an attenuance at 600 nm of 0.4 with 1 mM isopropyl β-D-thiogalactoside. Cells were incubated for a further 2 h prior to harvesting by centrifugation. Incubation in the presence of isopropyl β-D-thiogalactoside was at 42 °C for the variants of G2. After cell disruption by freeze-thawing and sonication in 20 mM Tris/HCl (pH 7.8)/1 mM EGTA (buffer A) and a cocktail of protease inhibitors (Complete, Boehringer Mannheim), the pellet of inclusion bodies was washed once with 0.5 % CHAPS, twice with 0.5 % Triton X-100, once with 2 M NaCl, once more with 0.5 % Triton X-100 (all solutions in buffer A) and finally once with buffer A alone. Inclusion bodies were solubilized in 8 M urea/20 mM dithiothreitol (DTT) in buffer A or in 20 mM Mes (pH 6)/1 mM EGTA (buffer B) in the case of G1–G2.

The two variants of G1 were applied on to a DEAE–Sepharose fast flow column (25 ml, Pharmacia) equilibrated with 8 M urea and 1 mM DTT in buffer A. After extensive washing with 1 mM DTT in buffer A without urea, the protein was eluted with a linear gradient of 0–300 mM NaCl, in the same buffer. The column was then re-equilibrated with 8 M urea in the same buffer and the washing and elution steps were repeated. This procedure was repeated five times until most of the protein had been eluted. Although both variants were obtained in soluble form, G1 (residues 37–133) was found to be aggregated by gel filtration. No further work was performed with this module.

The same procedure was applied to the two variants of G2, except that the resin was sulphopropyl (SP)-Sepharose (Pharmacia) and that three denaturation/renaturation/elution cycles were sufficient to obtain most of the protein.

The bimodule G1–G2 was first purified in 8 M urea on a SP-Sepharose column equilibrated in buffer B containing 8 M urea and 1 mM DTT. The protein was eluted with a linear gradient of 0–400 mM NaCl in the same urea-containing buffer. Renaturation was performed by rapid dilution. The protein was added drop-wise to 10 vols of 20 mM Tris/HCl (pH 7.8) containing 1 mM DTT, 0.4 mM $CaCl_2$ and 200 mM NaCl at 4 °C. After dialysis against the same buffer the protein was concentrated in an Amicon cell with a YM-10 membrane.

Protein concentrations were determined from the absorbance at 280 nm with the following calculated [19] extinction coefficients, ϵ_{280}: 20460 $M^{-1} \cdot cm^{-1}$ for G1 (37–150), 14180 $M^{-1} \cdot cm^{-1}$ for G2 (137–255), 12900 $M^{-1} \cdot cm^{-1}$ for G2 (152–255) and 33360 $M^{-1} \cdot cm^{-1}$ for G1–G2.

Oxidation of G2 and G1–G2 was achieved by overnight dialysis against the appropriate buffers without DTT.

Determination of free thiols

The concentration of free thiols was determined by the reaction of Ellman (see [20]). After gel filtration on a G-25 column (NAP-5, Pharmacia) to remove small-molecule thiols, the absorbance at 412 nm was measured with and without 6 M guanidinium chloride after addition of a one-ninteenth vol. of 3 mM 5,5′-dithiobis-(2-nitrobenzoic acid). The extinction coefficients $\epsilon =$ 14150 $M^{-1} \cdot cm^{-1}$ and $\epsilon =$ 13700 $M^{-1} \cdot cm^{-1}$ [20] were used in the absence and presence of guanidinium chloride, respectively.

Spectroscopic measurements

All measurements were performed at 25 °C in thermostat-controlled instruments. The buffer was 4 mM Tris/HCl, pH 7.8, containing 200 mM NaCl and 1 mM EGTA, with and without various concentrations of urea and 1 mM DTT. For measurements in the presence of calcium, $CaCl_2$ was added to a final concentration of 10 mM. Protein concentrations were 4 μM for G1, 6 μM for G2 (137–255), 15 μM for G2 (152–255) and 2.5 μM for G1–G2.

Fluorescence emission spectra were recorded in an Aminco-Bowman series 2 luminescence spectrometer. Excitation was at 280 nm. CD spectra were acquired in a Jobin-Yvon CD6 spectropolarimeter using 1- and 0.1-cm cuvettes for the near- and far-UV regions, respectively.

Gel filtration

Analytical gel filtration was performed at room temperature (23 °C) on a Superdex 200 HR size-exclusion column (30 × 1 cm; Pharmacia) at a flow rate of 0.8 ml/min, with buffer A containing 200 mM NaCl and either 1 mM EGTA or 10 mM $CaCl_2$, in the presence or absence of 1 mM DTT. Protein concentration was between 0.1 and 0.5 mg/ml. Calibration was performed with aprotinin, ribonuclease A, chymotrypsinogen A, ovalbumin and BSA.

Unfolding equilibria and Ca^{2+} titration

Urea-induced unfolding transitions were monitored by recording complete emission fluorescence spectra of protein solutions that had been incubated for at least 15 min in various concentrations of urea. Some samples were re-examined after 24 h to check that the equilibrium had been established. A number of samples were denatured in 8 M urea prior to dilution into buffers containing different concentrations of urea, in order to check that the unfolding reaction was fully reversible. Denaturant concentrations were calculated from the refractive indices of the samples [21]. CD spectra in the far-UV were recorded between 220 and 250 nm for some selected urea concentrations. Ca^{2+} titrations were carried out similarly by recording complete emission spectra at varying concentrations of $CaCl_2$ and a defined urea concentration. Data were analysed by non-linear least-squares fitting to the equations given in the Results section with the program Kaleidagraph.

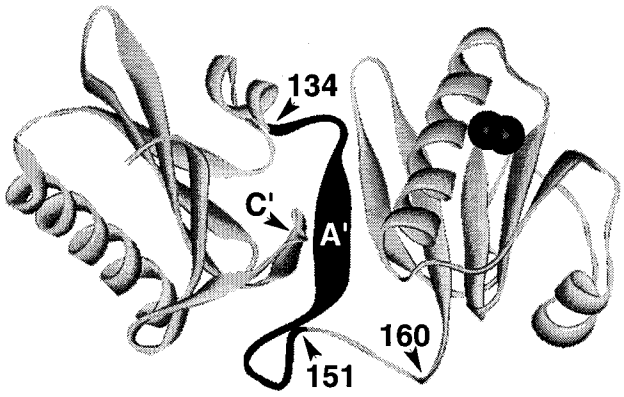

Figure 1 Ribbon representation of the bimodule G1–G2 (37–255) extracted from the crystallographic structure of equine plasma gelsolin [8]

Residues 134–151 are darkened to allow the visualization of the fragments G1 (37–133), G1 (37–150), G2 (137–255) and G2 (152–255). The sulphur atoms of the G2 disulphide bond are shown as spheres. The figure was prepared using WebLab ViewerPro (Molecular Simulations).

RESULTS

Choice of gelsolin fragments

Gelsolin modules consist of a five-stranded β-sheet (strands labelled A–E) sandwiched between a four-turn α-helix parallel to the β-strands, and 1.5-turn α-helix perpendicular to the β-strands [8]. In addition to these features, G1 and G2 are connected by 23 residues forming a β-strand (138–141) termed A′ and a loop (142–160; Figure 1). G1 also extends an additional loop between strands B and C, which comprises a short β-strand (C′). These β-strands (A′ and C′) continue the core β-sheet of G2. It is difficult to attribute the A′ β-strand to either module, as it appears structurally to belong to G2 in the absence of calcium [8], but was part of G1 in previous structural studies of this module [22]. We have made constructs for two variants of each module as well as the bimodule. G1 was produced as fragment 37–150, which contains the A′ β-strand and part of the long loop connecting to G2. Production of fragment 37–133, which does not contain the A′ β-strand, was not successful. Residues 1–36 were deleted, as they constitute an N-terminal extension not found in the other modules. G2 was produced as fragments 137–255, which contains the A′ strand and the intervening loop, and 152–255, which does not. The bimodule G1–G2 consisted of residues 37–255. G1 and G2 each contain two tryptophan residues. Trp-88 and Trp-200 are part of the conserved hydrophobic core and Trp-44 and Trp-180 are specific to G1 and G2, respectively.

Expression and purification

The four individual modules and the bimodule were greatly overexpressed in *E. coli*. The two variants of G1 and the bimodule G1–G2 were expressed solely as inclusion bodies. In contrast, the two variants of G2 were expressed at 37 °C, both in soluble form and as inclusion bodies, in comparable proportions. In order to facilitate the purification, the fraction of G2 in inclusion bodies was increased by inducing the expression at 42 °C.

After denaturation of the inclusion bodies, the variant G1 (37–150) was renatured on an anion-exchange resin DEAE–Sepharose. About 50 % of the protein could be eluted after the first renaturation. Decreasing amounts of G1 were eluted successively after each subsequent cycle of denaturation and renaturation on the resin. A likely explanation is that upon removal of the denaturant a fraction of the protein did not fold but aggregated in the column. The same approach was used to renature the two variants of G2, except that a cation-exchange resin SP-Sepharose was used. On the contrary, renaturation of the bimodule G1–G2 on ion-exchange resin was not successful. Refolding was achieved, after purification under denaturing conditions, by rapid dilution in a large volume of buffer containing 200 mM NaCl. The protein precipitated with lower salt concentrations, possibly explaining the failure of the chromatographic procedure. G1–G2 was stored at 4 °C as it was found to precipitate after freeze-thawing. The amount of purified protein obtained per litre of culture was 20–25 mg for the single modules and 6 mg for the bimodule. The correct identity of the fragments was checked by MS.

Table 1 Hydrodynamic volumes of gelsolin fragments determined by Superdex 200 gel filtration

S.E.s of the residuals of the calibration curve are shown. The S.E. between duplicate runs was 0 at the given level of precision. N.D., not determined.

	Oxidized		Reduced	
	$+Ca^{2+}$	$-Ca^{2+}$	$+Ca^{2+}$	$-Ca^{2+}$
G1 (37–150)	N.D.	N.D.	16.2 ± 0.1	18.6 ± 0.1
G2 (137–255)	18.2 ± 0.1	18.2 ± 0.1	18.5 ± 0.1	19.1 ± 0.1
G2 (152–255)	17.3 ± 0.1	17.3 ± 0.1	17.5 ± 0.1	17.7 ± 0.1
G1–G2 (37–255)	19.5 ± 0.1	20.2 ± 0.1	20.2 ± 0.1	23.7 ± 0.1

Hydrodynamic volume

Analytical gel filtration showed that the recombinant fragments were monomeric under all experimental conditions after renaturation from inclusion bodies (Table 1). G1 (37–150) was expanded by 15 % in the absence of Ca^{2+}. In contrast, the hydrodynamic volume of oxidized G2 was not affected by Ca^{2+}. Reduced G2, on the other hand, appeared only slightly larger in the presence of calcium, but it was significantly expanded in the absence of Ca^{2+}. Similarly, the absence or presence of calcium had a small effect on the volume of oxidized G1–G2, but the volume of the reduced form was increased by 17 % in the absence of Ca^{2+}.

Conformational stability

The conformational stability of the fragments was probed by measuring urea-induced unfolding equilibria, monitored by fluorescence. Equilibria were rapidly established, as there was no significant difference between measurements done 15 min or 24 h after mixing. Data from samples that were prepared by dilution from 0 or 8 M urea fell on the same curve, demonstrating that the reaction was reversible. The same transitions were also observed by CD in the far-UV (results not shown). For G1 and oxidized G2, data could be fitted according to a two-state model, by linear extrapolation of the free energy of folding, $\triangle G_F$, to zero concentration of denaturant [21] (Figures 2A and 2B):

$$\text{Fluorescence} = \{(a[\text{Urea}]+b)+(c[\text{Urea}]+d) \times \exp[(\triangle G^0_F - \triangle G^0_F[\text{Urea}]/C_M)/RT]\} \times \{1+exp[(\triangle G^0_F - \triangle G^0_F[\text{Urea}]/C_M)/RT]\}^{-1}$$

where $a[\text{Urea}]+b$ and $c[\text{Urea}]+d$ are the fluorescence of the native and unfolded forms, respectively, R is the gas constant

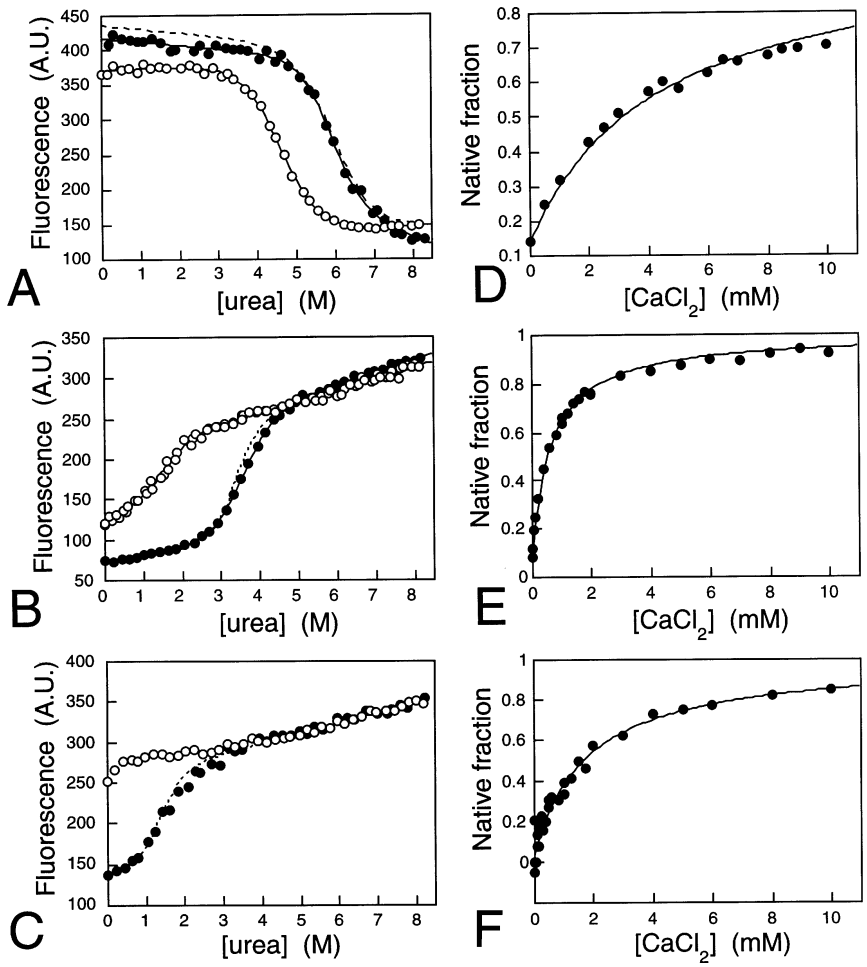

Figure 2 Urea-induced unfolding transitions and Ca^{2+} titrations of G1 (37–150) (A, D) and of oxidized (B, E) and reduced (C, F) G2 (152–255)

(**A**–**C**) Filled symbols were in the presence of 10 mM $CaCl_2$, open symbols were with 1 mM EGTA. Ca^{2+} titrations: G1 (37–150) at 5.5 M urea (**D**), oxidized G2 (152–255) at 2.5 M urea (**E**) and reduced G2 (152–255) at 0.7 M urea (**F**). The conformation was monitored by fluorescence at 320 nm for G1 (**A** and **D**) or 360 nm for G2 (**B**, **C**, **E** and **F**). The solid lines represent the non-linear least-square fits to the data; values are given in Table 2. The dashed lines represent simulations at 10 mM Ca^{2+} using parameters derived from the unfolding data in the presence of EGTA and the K_D for Ca^{2+} obtained from the titration data.

Table 2 Thermodynamic values for the urea-induced unfolding of G1 and G2 at pH 7.8 and 25 °C obtained by non-linear least-squares fitting of the data to a two-state model

	Ca^{2+}	C_M (M)	m (kcal·mol^{-1}·M^{-1})	ΔG_F^0 (kcal·mol^{-1})
G1 (37–150)	+	5.86 ± 0.06	1.4 ± 0.1	−8.4 ± 0.7
	−	4.60 ± 0.03	1.2 ± 0.1	−5.4 ± 0.2
G2 (137–255) oxidized	+	3.35 ± 0.05	1.5 ± 0.2	−5.2 ± 0.5
G2 (152–255) oxidized	+	3.51 ± 0.03	1.5 ± 0.1	−5.3 ± 0.3
	−	1.75 ± 0.12	1.9 ± 0.6	−3.4 ± 0.8

and T the temperature, and $\triangle G_F^0$ is the free energy of folding in the absence of denaturant. The linear dependence of $\triangle G_F$ on the concentration of denaturant is described by: $\triangle G_F = \triangle G_F^0 + m[\text{Urea}]$, where $m = -\triangle G_F^0/C_M$ and C_M is the concentration of urea corresponding to the mid-point of the folding transition.

Analysis of the unfolding data at different wavelengths yielded the same values of C_M, m and $\triangle G_F^0$, within the margin of error, supporting the validity of the two-state model. The results given in Table 2 show that 10 mM calcium provides a stabilization of 3.0 ± 0.9 kcal·mol^{-1} to G1 (37–150) and 1.9 ± 1.2 kcal·mol^{-1} to G2 (152–255). They also indicate that G1 is more stable than G2 by about 2 kcal·mol^{-1} in the absence of calcium and that the 15 additional residues of G2 (137–255) comprising the A′ β-strand do not significantly contribute to the conformational stability of G2.

The unfolding of reduced G2 in the presence of Ca^{2+} displays one transition between 1 and 2 M urea with an approximate mid-point at 1.5 M (Figure 2C). Although the values of $\triangle G_F^0$, C_M and m could not be extracted from the data, the lower C_M and the reduced slope of the transition (smaller m) indicates that reduced G2 is destabilized relative to the oxidized form at zero concentration of denaturant. In the absence of Ca^{2+}, reduced G2 exhibits a single transition between 0 and 0.5 M urea (Figure 2C). However, the protein appears to be largely unfolded in the absence of urea, and only a partial transition is observed. Assuming that G2 in the presence of 10 mM Ca^{2+} is fully folded

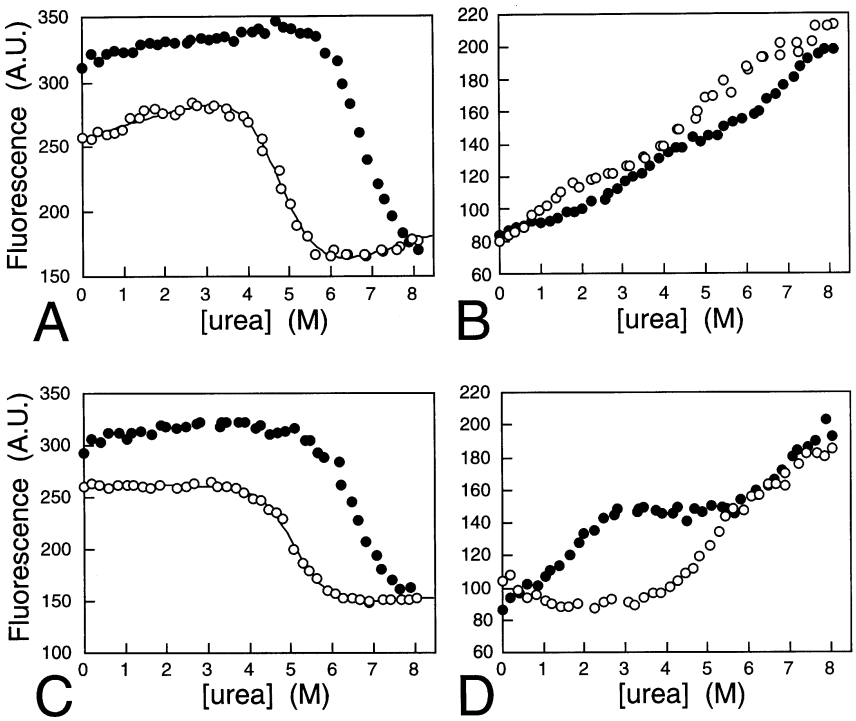

Figure 3 Urea-induced unfolding transitions of oxidized (A and B) and reduced (C and D) G1–G2 (37–255) monitored by fluorescence at 320 nm (A and C) and 360 nm (B and D)

Symbols and conditions are as in Figure 2.

and that the fluorescence of native calcium-free G2 is the same as that of calcium-bound G2, the fluorescence at zero concentration of denaturant indicates that G2 without calcium is about 80% non-native, which translates into a rough estimate for $\triangle G^0_F$ of about $+1$ kcal·mol^{-1}.

To estimate the dissociation constant for calcium (K_D), the fluorescence was measured with varying concentrations of Ca^{2+} at a urea concentration at which most of the protein is folded in the presence of calcium and unfolded in its absence (Figures 2D–2F). For G1 and oxidized G2, the native fraction at 0 and 10 mM Ca^{2+} was calculated at the chosen urea concentration using the parameters given in Table 2. For reduced G2, the native fraction at 0 mM Ca^{2+} was taken as zero, and the value at 10 mM Ca^{2+} was estimated from Figure 2C. These values were used to normalize the fluorescence data into native-fraction values at various Ca^{2+} concentrations. These values were fitted to the following equation:

$$\text{Native fraction} = (1+[Ca^{2+}]/K_D)\{1+[Ca^{2+}]/K_D + \exp[(\triangle G^0_F - \triangle G^0_F[\text{Urea}]/C_M)/RT]\}^{-1}$$

where $\triangle G^0_F$ and m are the thermodynamic parameters for the folding of the calcium-free protein and [Urea] is the chosen urea concentration. For G1 and oxidized G2, $\triangle G^0_F$ and m were obtained from the fit of Figures 2(A) and 2(B) and are given in Table 2. For reduced G2, the estimated $\triangle G^0_F$ of $+1$ kcal·mol^{-1} was used together with $m = 1.9$ kcal·mol^{-1}·M^{-1}, assumed to be equal to that of calcium-free oxidized G2. Using the above equation assumes that the fluorescence of the calcium-bound and calcium-free native forms are the same or that the amount of calcium-free native form is negligible. The following K_D values were obtained: 630 ± 20 μM for G1, 50 ± 1 μM for oxidized G2 and 32 ± 4 μM for reduced G2.

Table 3 Estimated transition range and C_M for the urea-induced unfolding of G1–G2 (37–255) at pH 7.8 and 25 °C

	Wavelength (nm)	Range of transition (M) urea	Estimated C_M (M) urea
Oxidized $+Ca^{2+}$	360	2.4–4.4	3.5
	320 + 360	5.8–8.0	6.8
Oxidized $-Ca^{2+}$	360	0.5–2.0	1.3
	320 + 360	3.8–6.0	4.8
Reduced $+Ca^{2+}$	360	0.0–2.6	1.6
	320 + 360	5.4–8.0	6.8
Reduced $-Ca^{2+}$	360	0.0–1.0	0.5
	320 + 360	3.8–6.4	5.0

Reversibility of the unfolding reaction was also observed for G1–G2 despite the fact that, under denaturing conditions, the disulphide bond of G2 can probably rearrange to some extent with the free thiol of Cys-93 of G1. Two transitions were observed for all four forms of the bimodule, most probably corresponding to unfolding of the two modules (Figure 3). The range of urea concentrations and the estimated mid-points of transitions are summarized in Table 3.

Despite a greater amplitude of the unfolding signal at 320 nm than at 360 nm, the first transition at low concentration of denaturant was observed only at the latter wavelength. By comparison with the transitions of the single modules, the transition at low urea concentration can be attributed to unfolding of G2 and that at high urea concentration to unfolding of G1. If the approximate mid-points of transition are taken as

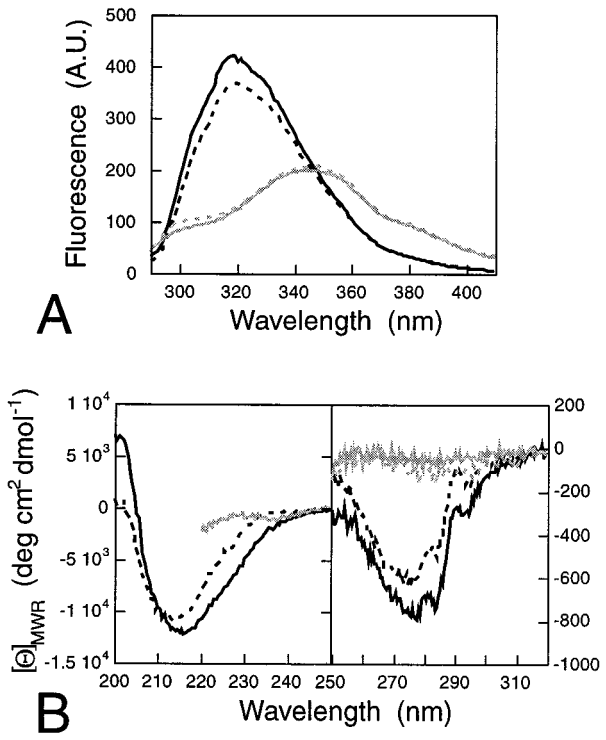

Figure 4 Spectroscopic characterization of G1 (37–150) at pH 7.8 and 25 °C

Fluorescence emission spectra with excitation at 280 nm (**A**) and CD spectra (**B**). Black and grey lines represent the absence and the presence of 8 M urea, respectively. Solid lines indicate the presence of 10 mM $CaCl_2$ and dashed lines the presence of 1 mM EGTA.

a measure of the relative stability of the modules, the stabilization gained by G2 being part of the bimodule G1–G2 is marginal. Only for the reduced form, in the absence of Ca^{2+}, was there a noticeable stabilizing effect of the bimodule on G2, although the small amplitude of the transition renders this estimation difficult. The conformation of G1 appears to be slightly more stable as part of the bimodule. This, however, could be due to a proximal effect of the additional sequence on the C-terminus of G1, rather than to an interaction with G2.

Spectroscopic characterization and thiol reactivity

Fluorescence emission and CD spectra were measured in order to detect structural modifications that could be correlated with the changes of stability caused by Ca^{2+} and the disulphide bond. Fluorescence spectra of G1 (37–150) showed emission maxima at 318 and 319 nm, in the presence and absence of Ca^{2+} respectively, indicating that both tryptophan residues are largely protected from the aqueous environment (Figure 4A). The CD signal in the near-UV region also revealed that the aromatic residues were in a folded environment, without significant differences due to Ca^{2+} (Figure 4B). In contrast, the CD spectra in the far-UV region, which are dominated by β-sheet signal, were significantly different in the presence and absence of Ca^{2+}, with minima at 215 and 213 nm, respectively (Figure 4B). The protein appears to be more structured in the presence of Ca^{2+}.

Fluorescence spectra of oxidized G2 showed emission maxima at 321 nm in the presence of $Ca^{2+}$and 330 nm in its absence

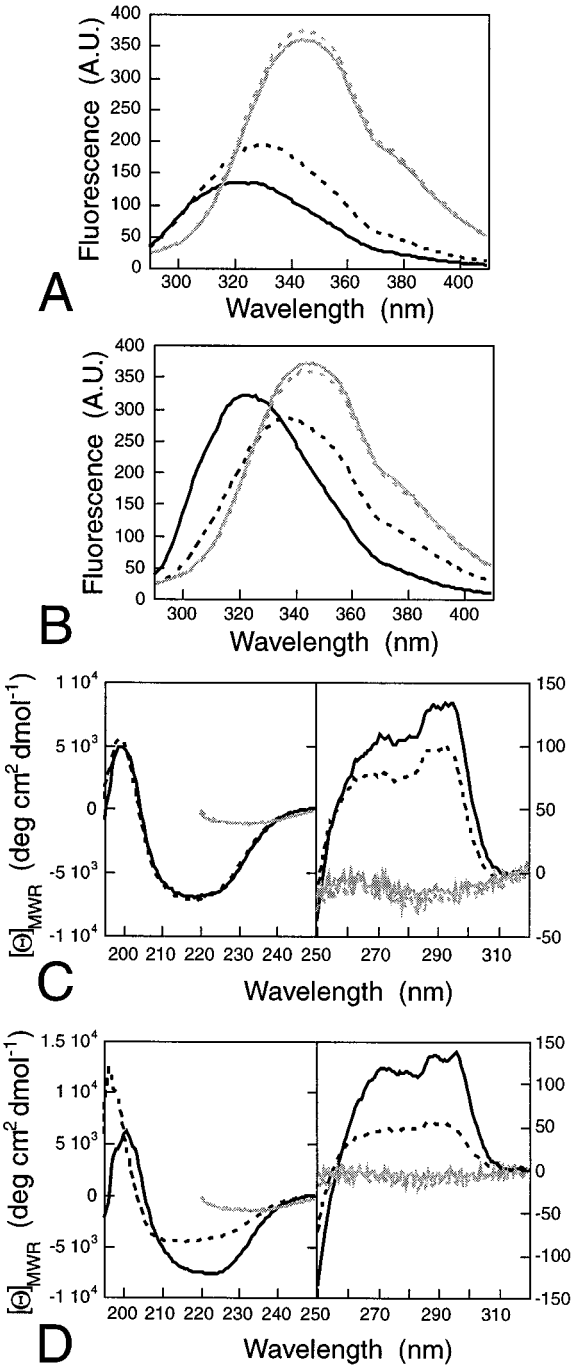

Figure 5 Spectroscopic characterization of G2 (152–255)

Fluorescence emission spectra with excitation at 280 nm of the oxidized (**A**) and reduced (**B**) forms, and CD spectra of the oxidized (**C**) and reduced (**D**) forms. Symbols and conditions are as given in Figure 4.

(Figure 5A). The intensity of fluorescence was reduced compared with the unfolded forms in the presence of 8 M urea. The fluorescence intensity of the reduced forms was higher and comparable with that of the unfolded forms (Figure 5B). The emission maximum was at 322 nm with Ca^{2+}, but was significantly red-shifted to 337 nm in the absence of calcium. These important shifts indicate that one or both tryptophan residues of G2 are

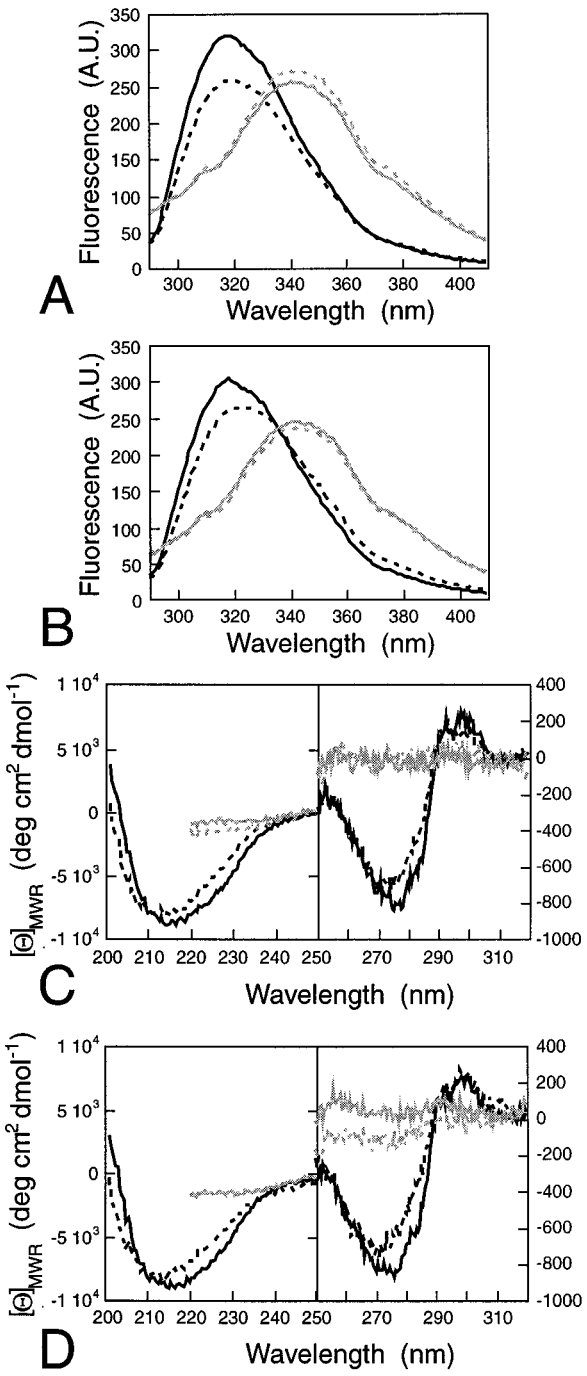

Figure 6 Spectroscopic characterization of G1–G2 (37–255)

Fluorescence emission spectra with excitation at 280 nm of the oxidized (**A**) and reduced (**B**) forms, and CD spectra of the oxidized (**C**) and reduced (**D**) forms. Symbols and conditions are as given in Figure 4.

more exposed to the solvent in the absence of Ca^{2+}. This is particularly the case in reduced G2, which has a spectrum close to that of the denatured fragment. CD spectra of G2 in the near-UV region showed little variation between the oxidized and reduced forms, in the presence of Ca^{2+} (Figures 5C and 5D). Oxidized G2 without Ca^{2+} had a very similar spectrum as well (Figure 5C). Only the reduced form in the absence of Ca^{2+} had a significantly lowered CD signal, particularly between 285 and 300 nm (Figure 5D).

In the far-UV region, the CD signal of G2 differs substantially from that of G1 (compare Figure 4B with Figures 5C and 5D), which is somewhat unexpected considering that they have similar topologies and secondary structures. The oxidized forms have minima at 216 nm, but with a largely flat signal between 210 and 225 nm. In comparison with G1, this would suggest a greater contribution of α-helices to the secondary structure of G2. No spectral differences in the far-UV could be noted in the presence or absence of Ca^{2+} for the oxidized forms (Figure 5C). In contrast, the reduced form showed a marked reduction of CD signal in the absence of Ca^{2+}, with a shift of the minimum from 222 nm with Ca^{2+} to 209 nm without, suggesting a partial loss of secondary structure, particularly of α-helices (Figure 5D).

Titration of the free thiols of G2 (137–255) by Ellman's reaction, under denaturing conditions, demonstrated that the disulphide bond between Cys-188 and Cys-201 had been formed after dialysis against a buffer devoid of reducing agent. Conversely, incubation of the folded protein with 1 mM DTT achieved complete reduction of the disulphide bond. Under non-denaturing conditions in the presence of Ca^{2+}, however, only a little more than 1 mol of thiol per mol of reduced G2 reacted rather slowly, indicating that one of the thiols was inaccessible to the reagent. In contrast, in the absence of Ca^{2+}, the kinetics of the reaction under native conditions revealed that the two thiols of the reduced form are accessible and very reactive towards the reagent.

The fluorescence and near-UV CD spectra and the accessibility of the thiols indicate that reduced G2 loses the tight packing of its hydrophobic core in the absence of Ca^{2+}, whereas the CD signal in the far-UV indicates the retention of some secondary structure. Thus the non-native conformation adopted by calcium-free reduced G2 qualifies as molten globule.

The fluorescence spectra of the oxidized forms of G1–G2 were indicative of the protection of the tryptophan residues from the aqueous solvent with emission maxima at 317 and 318 nm in the presence and absence of Ca^{2+} respectively (Figures 6A and 6B). The spectrum of the reduced form in the presence of Ca^{2+} was similar with a maximum at 318 nm. In contrast, in the absence of Ca^{2+}, the maximum was red-shifted with an emission maximum at 323 nm, suggesting the greater exposure of at least one of the tryptophan residues. In contrast to what was observed with G2 alone, the oxidized forms exhibited a greater intensity of fluorescence than the reduced forms.

The CD spectra in the near- and far-UV regions were similar for the reduced and oxidized forms, with few differences due to the presence or absence of Ca^{2+} (Figures 6C and 6D). In the near-UV, the shape of the spectra suggested that they result from the simple addition of the spectra of both individual modules. It is somewhat surprising that the shift of fluorescence emission maximum of the reduced form in the absence of Ca^{2+}, as well as the change of hydrodynamic volume (Table 1), did not translate into a modification of the CD spectrum. In both the near- and far-UV, the differences observed between the spectra of the reduced forms of G2, with and without calcium, were not observed with the bimodule G1–G2. This shows that Ca^{2+}-free reduced G2 is stabilized and more folded in the bimodule than individually.

DISCUSSION

Gelsolin is most unusual in that it functions both intra- and extracellularly. The secreted form is presumably constitutively activated by calcium and contains a disulphide bond, while the cytoplasmic form is regulated by variations of Ca^{2+} concentration and has reduced cysteines [7,23]. Plasma gelsolin in the absence

of calcium has a compact structure with the six modules making intimate contacts and masking the actin-binding sites [8]. Binding of calcium ions is thought to induce a large conformational change, thus unmasking the actin-binding sites. The change of conformation upon calcium binding has been documented by the sensitivity to proteolysis, UV difference spectroscopy, CD spectroscopy, ultracentrifugation, intrinsic and extrinsic fluorescence, free thiol titration, dynamic light scattering and X-ray crystallography [9,24–29]. At least three Ca^{2+}-binding sites have been found in actin-free gelsolin. One is shared by G4 and G5 with a dissociation constant, K_D, of 2 μM, and a second one by G5 and G6 with a dissociation constant of 0.2 μM [30]. One Ca^{2+}-binding site is also found in the triplet G1–G3 with a dissociation constant of 0.2 μM [30]. This site might be the same high-affinity Ca^{2+}-binding site found in G1 complexed with G-actin at neutral pH [22,31]. However, the affinity of G1 alone for Ca^{2+} is very low with an estimated dissociation constant of 3 mM [31]. On the other hand, earlier measurements of Ca^{2+} binding to truncated gelsolins suggested that the Ca^{2+} bound by G1–G3 was localized in the G2–G3 bimodule [32]. Susceptibility to proteolysis and change of molecular volume have also suggested that a calcium-binding site was present in G2–G3 [24]. G2 itself, however, does not require Ca^{2+} to interact with F-actin [33].

The present study is the first report, to our knowledge, of calcium binding by G2 isolated or within the bimodule G1–G2. Without its disulphide bond, isolated G2 is not fully folded in the absence of calcium. The Ca^{2+}-binding site reported for the bimodule G2–G3 [24] is then certainly comprised within the fragment G2 (152–255). The Ca^{2+}-binding site of G5–G6 [30], which has not been identified in the structure of actin- and Ca^{2+}-bound G4–G6 [9], might similarly be located in G5.

The plasma form of gelsolin must fold in the endoplasmic reticulum where it enters the secretory pathway. The free calcium concentration in the endoplasmic reticulum is thought to be in the range of 0.5–1 mM [10]. The calcium concentration is also high in the extracellular medium. Under these conditions gelsolin must be activated constitutively. The dissociation constant for Ca^{2+} and oxidized G2 was estimated to be 50 μM, indicating that secreted G2 is certainly calcium-bound.

A dissociation constant of 30 μM was found for Ca^{2+} and reduced G2, suggesting that an isolated G2 in the cytoplasm, where the free calcium concentration is in the low-micromolar range, would not bind Ca^{2+}. However, this value must be considered as tentative as the parameters used for its calculation were rough estimates ($\triangle G^0_F$ and m). Stability studies of G2 (151–266), in which neither calcium nor EGTA were added to the reaction mixture, found that reduced G2 was folded [34]. It is possible that the additional 11 C-terminal residues of this construct provide additional stabilizing interactions.

G2 in the cytoplasm may never exist without interacting with other parts of gelsolin, in particular G1 and G6 [8], with F-actin [33] or with PtdIns(4,5)P_2 [35]. PtdIns(4,5)P_2 is known to bind to the segment 150–169 of G2 and to inhibit gelsolin activity. Each of these interactions may stabilize the native conformation of G2 in the cytoplasm where the disulphide bond is not formed and the Ca^{2+} concentration is low. In the absence of stabilizing interactions with other modules, F-actin or PtdIns(4,5)P_2, as in the secreted form, G2 might require the extra stabilization provided by Ca^{2+} or the disulphide bond.

In vivo, the absence of disulphide bond in G2, obtained by site-directed mutagenesis, resulted in an intracellular proteolytic processing similar to that observed in familial amyloidosis Finnish type [36]. It was therefore proposed that the amyloidogenic mutations at Asp-187 could prevent the formation of the disulphide bond between the adjacent Cys-188 and Cys-201. Recombinant modules G2 with Asp-187 replaced by either Asn or Tyr were found to form the disulphide bond [33]. However, formation of a disulphide bond under aerobic conditions does not mean that it is stable at the redox potential of the endoplasmic reticulum. The relative stability of the disulphide bond in the mutant forms of G2 will have to be measured to resolve this issue.

The present work shows that the absence of disulphide bond between Cys-188 and Cys-201 destabilizes G2. This destabilization could result in the increased susceptibility to proteolysis observed *in vivo* [36]. This result, however, does not imply that the absence of the disulphide bond is the cause of the proteolytic processing that occurs with amyloidogenic mutants. Other destabilizing factors could have the same consequence, as the replacement of Asp-187 by Asn or Tyr was also found to destabilize G2 [33]. The destabilization has been attributed to the disruption of a network of hydrogen bonds that involves Asp-187, Gln-164, Lys-166 and Asn-184 [8,33]. The stabilization provided by Ca^{2+} suggests another explanation for the effect of the amyloidogenic mutations, as the carboxylate of Asp-187 could contribute to the Ca^{2+}-binding site. Its replacement would suppress an important stabilizing factor in the secretory pathway and the plasma, while the cytoplasmic form would be largely unaffected as G2 could be stabilized by other multiple interactions. This hypothesis could be tested by investigating the effect of Ca^{2+} on the stability of amyloidogenic mutants of G2.

The marginal stability of G2 might explain the variation of hydrodynamic volume between various truncated gelsolins. It was found that the volumes of whole gelsolin and of a G2–G6 construct were greater in the presence of calcium, which was interpreted as the opening of the molecule following disruption of the interaction between G2 and G6. In contrast, G1–G3 and G1–G5 constructs have greater volumes in the absence than in the presence of Ca^{2+} [24]. These observations could be due to partial unfolding of G2 rather than an intermodular rearrangement. That G2 is less compact in the absence of Ca^{2+} has also been shown by increased susceptibility to proteolysis by plasmin in constructs G2–G3, G1–G3 and G1–G5 [24]. Cleavage occurred between residues 228 and 229. The same site is cleaved by plasmin in whole gelsolin in the absence of Ca^{2+}, but only in the absence of disulphide bond [24].

G1 is also shown to be stabilized by Ca^{2+} and to undergo a structural modification upon Ca^{2+} binding. Although several studies failed to observe Ca^{2+} binding by this isolated module, it might be simply the consequence of the very low affinity [31]. Indeed, titration at a urea concentration that was denaturing for Ca^{2+}-free G1 but non-denaturing for Ca^{2+}-bound G1 yielded a dissociation constant of 0.6 mM. The structural change observed by far-UV CD spectroscopy could be due to the rearrangement of the C-terminus of G1 (37–150). Comparison of the structures of Ca^{2+}-free gelsolin and the Ca^{2+}-bound G1–actin complex suggested that Ca^{2+} binding causes a reorientation of the main chain, as the carbonyl of Val-145 is flipped by 180 ° to coordinate the Ca^{2+} ion [8,22]. This local change could affect the loop (142–150) and the A′ β-strand (138–141), as well as the short C′ β-strand, which forms a small β-sheet with A′.

Despite the extensive contacts between G1 and G2 observed in the crystallographic structure in the absence of Ca^{2+}, only a marginal stabilization was observed in the bimodule G1–G2. However, this stabilization was sufficient to confer a more native-like conformation on G2, as judged by CD and fluorescence spectroscopy. When the individual G1 and G2 were mixed at micromolar concentrations, no association could be detected by gel filtration, even in the absence of Ca^{2+} (results not shown). This indicates that more interactions are required to

stabilize the conformation of G1–G2 as found in whole Ca^{2+}-free gelsolin. These interactions could be the contact between G2 and the C-terminal helix of G6 or the restriction of freedom imposed on G2, through the long stretch connecting G2 and G3, by the binding of G3 on the opposite side of G1.

The present work demonstrates that modules that evolved from a common ancestor can differ in their intrinsic stability and their stabilizing factors. Moreover, these stabilizing factors may be different for the same module, depending on its physiological location.

We thank Helen L. Yin for providing the gelsolin cDNA, Robert C. Robinson for supplying co-ordinates of equine gelsolin and Michel Jacquinot for performing the MS measurements. This work was supported by the Physique et Chimie du Vivant programme of CNRS.

REFERENCES

1 Kwiatkowski, D. J. (1999) Functions of gelsolin: motility, signaling, apoptosis, cancer. Curr. Opin. Cell Biol. **11**, 103–108
2 Azuma, T., Witke, W., Stossel, T. P., Hartwig, J. H. and Kwiatkowski, D. J. (1998) Gelsolin is a downstream effector of rac for fibroblast motility. EMBO J. **17**, 1362–1370
3 Kothakota, S., Azuma, T., Reinhard, C., Klippel, A., Tang, J., Chu, K., McGarry, T. J., Kirschner, M. W., Koths, K., Kwiatkowski, D. J. and Williams, L. T. (1997) Caspase-3-generated fragment of gelsolin: effector of morphological change in apoptosis. Science **278**, 294–298
4 Lee, W. M. and Galbraith, R. M. (1992) The extracellular actin-scavenger system and actin toxicity. N. Engl. J. Med. **326**, 1335–1341
5 Yin, H. L. (1987) Gelsolin: calcium- and polyphosphoinositide-regulated actin-modulating protein. Bioessays **7**, 176–179
6 Kwiatkowski, D. J., Stossel, T. P., Orkin, S. H., Mole, J. E., Colten, H. R. and Yin, H. L. (1986) Plasma and cytoplasmic gelsolins are encoded by a single gene and contain a duplicated actin-binding domain. Nature (London) **323**, 455–458
7 Wen, D., Corina, K., Chow, E. P., Miller, S., Janmey, P. A. and Pepinsky, R. B. (1996) The plasma and cytoplasmic forms of human gelsolin differ in disulfide structure. Biochemistry **35**, 9700–9709
8 Burtnick, L. D., Koepf, E. K., Grimes, J., Jones, E. Y., Stuart, D. I., McLaughlin, P. J. and Robinson, R. C. (1997) The crystal structure of plasma gelsolin: implications for actin severing, capping, and nucleation. Cell **90**, 661–670
9 Robinson, R. C., Mejillano, M., Le, V. P., Burtnick, L. D., Yin, H. L. and Choe, S. (1999) Domain movement in gelsolin: a calcium-activated switch. Science **286**, 1939–1942
10 Meldolesi, J. and Pozzan, T. (1998) The endoplasmic reticulum Ca^{2+} store: a view from the lumen. Trends Biochem. Sci. **23**, 10–14
11 Jaenicke, R. (1999) Stability and folding of domain proteins. Progr. Biophys. Mol. Biol. **71**, 155–241
12 de la Chapelle, A., Tolvanen, R., Boysen, G., Santavy, J., Bleeker-Wagemakers, L., Maury, C. P. and Kere, J. (1992) Gelsolin-derived familial amyloidosis caused by asparagine or tyrosine substitution for aspartic acid at residue 187. Nat. Genet. **2**, 157–160
13 Kiuru, S. (1998) Gelsolin-related familial amyloidosis, Finnish type (FAF), and its variants found worldwide. Amyloid **5**, 55–66
14 Kangas, H., Ulmanen, I., Paunio, T., Kwiatkowski, D. J., Lehtovirta, M., Jalanko, A. and Peltonen, L. (1999) Functional consequences of amyloidosis mutation for gelsolin polypeptide – analysis of gelsolin-actin interaction and gelsolin processing in gelsolin knock-out fibroblasts. FEBS Lett. **454**, 233–239

Received 28 February 2000/23 June 2000; accepted 13 July 2000

15 Kangas, H., Paunio, T., Kalkkinen, N., Jalanko, A. and Peltonen, L. (1996) *In vitro* expression analysis shows that the secretory form of gelsolin is the sole source of amyloid in gelsolin-related amyloidosis. Hum. Mol. Genet. **5**, 1237–1243
16 Maury, C. P. (1991) Gelsolin-related amyloidosis. Identification of the amyloid protein in Finnish hereditary amyloidosis as a fragment of variant gelsolin. J. Clin. Invest. **87**, 1195–1199
17 Yu, F. X., Zhou, D. M. and Yin, H. L. (1991) Chimeric and truncated gCap39 elucidate the requirements for actin filament severing and end capping by the gelsolin family of proteins. J. Biol. Chem. **266**, 19269–19275
18 Kunkel, T. A. (1985) Rapid and efficient site-specific mutagenesis without phenotypic selection. Proc. Natl. Acad. Sci. U.S.A. **82**, 488–492
19 Pace, C. N., Vajdos, F., Fee, L., Grimsley, G. and Gray, T. (1995) How to measure and predict the molar absorption coefficient of a protein. Protein Sci. **4**, 2411–2423
20 Riddles, P. W., Blakeley, R. L. and Zerner, B. (1983) Reassessment of Ellman's reagent. Methods Enzymol. **91**, 49–60
21 Pace, C. N. (1986) Determination and analysis of urea and guanidine hydrochloride denaturation curves. Methods Enzymol. **131**, 266–280
22 McLaughlin, P. J., Gooch, J. T., Mannherz, H. G. and Weeds, A. G. (1993) Structure of gelsolin segment 1-actin complex and the mechanism of filament severing. Nature (London) **364**, 685–692
23 Sun, H. Q., Yamamoto, M., Mejillano, M. and Yin, H. L. (1999) Gelsolin, a multifunctional actin regulatory protein. J. Biol. Chem. **274**, 33179–33182
24 Pope, B. J., Gooch, J. T. and Weeds, A. G. (1997) Probing the effects of calcium on gelsolin. Biochemistry **36**, 15848–15855
25 Rouayrenc, J. F., Fattoum, A., Mejean, C. and Kassab, R. (1986) Characterization of the Ca^{2+}-induced conformational changes in gelsolin and identification of interaction regions between actin and gelsolin. Biochemistry **25**, 3859–3867
26 Reid, S. W., Koepf, E. K. and Burtnick, L. D. (1993) Fluorescent responses of acrylodan-labeled plasma gelsolin. Arch. Biochem. Biophys. **302**, 31–36
27 Kilhoffer, M. C. and Gerard, D. (1985) Fluorescence study of brevin, the Mr 92 000 actin-capping and -fragmenting protein isolated from serum. Effect of Ca^{2+} on protein conformation. Biochemistry **24**, 5653–5660
28 Koepf, E. K. and Burtnick, L. D. (1993) Horse plasma gelsolin labelled with fluorescein isothiocyanate responds to calcium and actin. Eur. J. Biochem. **212**, 713–718
29 Hellweg, T., Hinssen, H. and Eimer, W. (1993) The Ca(2+)-induced conformational change of gelsolin is located in the carboxyl-terminal half of the molecule. Biophys. J. **65**, 799–805
30 Pope, B., Maciver, S. and Weeds, A. (1995) Localization of the calcium-sensitive actin monomer binding site in gelsolin to segment 4 and identification of calcium binding sites. Biochemistry **34**, 1583–1588
31 Weeds, A. G., Gooch, J., McLaughlin, P., Pope, B., Bengtsdotter, M. and Karlsson, R. (1995) Identification of the trapped calcium in the gelsolin segment 1-actin complex: implications for the role of calcium in the control of gelsolin activity. FEBS Lett. **360**, 227–230
32 Way, M., Gooch, J., Pope, B. and Weeds, A. G. (1989) Expression of human plasma gelsolin in *Escherichia coli* and dissection of actin binding sites by segmental deletion mutagenesis. J. Cell Biol. **109**, 593–605
33 Way, M., Pope, B. and Weeds, A. G. (1992) Evidence for functional homology in the F-actin binding domains of gelsolin and alpha-actinin: implications for the requirements of severing and capping. J. Cell Biol. **119**, 835–842
34 Isaacson, R. L., Weeds, A. G. and Fersht, A. R. (1999) Equilibria and kinetics of folding of gelsolin domain 2 and mutants involved in familial amyloidosis-Finnish type. Proc. Natl. Acad. Sci. U.S.A. **96**, 11247–11252
35 Janmey, P. A., Lamb, J., Allen, P. G. and Matsudaira, P. T. (1992) Phosphoinositide-binding peptides derived from the sequences of gelsolin and villin. J. Biol. Chem. **267**, 11818–11823
36 Paunio, T., Kangas, H., Heinonen, O., Buc-Caron, M. H., Robert, J. J., Kaasinen, S., Julkunen, I., Mallet, J. and Peltonen, L. (1998) Cells of the neuronal lineage play a major role in the generation of amyloid precursor fragments in gelsolin-related amyloidosis. J. Biol. Chem. **273**, 16319–16324